

Ultrastructural elastic deformation of cortical bone tissue probed by NIR Raman spectroscopy.

William F. Finney^a, Michael D. Morris^{a*}, Joseph M. Wallace^{b,c}, David H. Kohn^{b,c}

^aDepartment of Chemistry, University of Michigan, Ann Arbor, MI USA 48109-1055

^bDepartment of Biologic and Materials Sciences University of Michigan, Ann Arbor, MI USA
48109-1078

^cDepartment of Biomedical Engineering, University of Michigan, Ann Arbor, MI USA 48109-2099

ABSTRACT

Raman spectroscopy is used as a probe of ultrastructural (molecular) changes in both the mineral and matrix (protein and glycoprotein, predominantly type I collagen) components of murine cortical bone as it responds to loading in the elastic regime. At the ultrastructural level, crystal structure and protein secondary structure distort as the tissue is loaded. These structural changes are followed as perturbations to tissue spectra. We load tissue in a custom-made dynamic mechanical tester that fits on the stage of a Raman microprobe and can accept hydrated tissue specimens. As the specimen is loaded in tension and/or compression, the shifts in mineral P-O₄ v₁ and relative band heights in the Amide III band envelope are followed with the microprobe. Average load is measured using a load cell while the tissue is loaded under displacement control. Changes occur in both the mineral and matrix components of bone as a response to elastic deformation. We propose that the mineral apatitic crystal lattice is deformed by movement of calcium and other ions. The matrix is proposed to respond by deformation of the collagen backbone. Raman microspectroscopy shows that bone mineral is not a passive contributor to tissue strength. The mineral active response to loading may function as a local energy storage and dissipation mechanism, thus helping to protect tissue from catastrophic damage.

Keywords: Raman, bone, biomechanics

1. INTRODUCTION

Raman spectroscopy has long been applied to the study of changes in the molecular structure of polymers, inorganic crystals and composite materials subjected to mechanical loads. Vibrational spectra of materials are sensitive to changes in such mineral parameters such as crystal structure, crystallite size and deviations from stoichiometry. Hence, changes in bond lengths, bond angles, internal rotation angles and the corresponding force constants can be monitored through measuring changes in the frequency, intensity and width of Raman bands. Raman spectroscopy is already an established technique for studying fatigue and damage in such materials as ceramics, semiconductors, and diamond films¹⁻⁴. Stress and strain mapping is an important application of Raman spectroscopy¹⁻⁸

Stress is the force applied to a specimen per unit of cross sectional area, typically reported in megaPascals (MPa) or gigaPascals (GPa). Strain is the change in length of the specimen per unit length of the specimen and is a dimensionless quantity. The most commonly used unit of strain in biological materials studies is microstrain, a change in unit length per million unit lengths. For small or oddly shaped specimens, where the attachment of strain gauges is difficult, measurement of the crosshead displacement, or the change in distance between the ends of the mechanical testing apparatus that support the specimen, suffices for an approximation of strain⁹. In many materials strain induces small frequency shifts in one or more Raman spectral bands. Often measurements are made under elastic deformation conditions, where there is likely to be a linear relationship between strain and band shift. Under elastic conditions observed changes in the specimen are presumed to be reversible and the relationship between applied load and strain is linear.

The properties of bone, because it is a composite material, are dependent on the architecture of the material at several dimensional scales, on interactions between the mineral and organic matrix and on the properties of each individual constituent.¹⁰ Bone is also hierarchical in structure and any study of bone must include investigation of the tissue at

*mdmorris@umich.edu; phone 1 734 764 7360; fax 1 734 615 3790

several levels of organization. Most biomechanical studies have studied the effect of mechanical load on bone tissue at macroscopic levels of architecture¹¹⁻¹⁸. We have previously shown that there are spectroscopically observable changes that occur in bone mineral and matrix associated with mechanical stress and deformation.¹⁹⁻²² These stresses range from microcracking to catastrophic failure, at dimensional scales ranging from tens of microns to several millimeters. Experiments with a cylindrical indenter have shown that these changes are the result of the mechanical stress, not preferential deformation at defects or specific variants in the composition of the bone material.²² Using high pressure Raman spectroscopy it has been shown that reversible changes occur to the mineral phase of bone tissue when it is subjected to hydrostatic pressures in excess of 3GPa.²³ We have also shown that deformation of bone mineral crystallites occurs when it is subjected to mechanical loads that are clearly in the physiological range²⁴ IR and Raman spectroscopy have been successfully used to study bone tissue.²⁵⁻³¹ The high spatial resolution and ability to work with thick, hydrated specimens make Raman spectroscopy a particularly advantageous approach. In Raman spectroscopy the phosphate ν_1 band envelope at ca. 960 cm^{-1} and the ca. 1070 cm^{-1} carbonate ν_1 /phosphate ν_3 band are useful markers for the investigation of the mineral component of bone. Changes in bone matrix, primarily type I collagen, can be monitored with the Amide I band envelope at ca. 1670 cm^{-1} and other protein bands such as Amide III band envelope at ca. 1240 cm^{-1} .

We here report our most recent results in our investigations of the molecular effects of mechanical loading in the elastic regime on intact mouse femora. We seek to determine if both the mineral and matrix contribute to the active response of bone to mechanical loads or if bone mineral is a passive contributor to the strength by using near real time collection of Raman spectroscopic data during mechanical loading. Changes in the phosphate ν_1 band as well as changes in the amide III band are observed under both tensile and compressive loading.

2. METHODOLOGY

Femora from 3-4 month old, female, C57Bl6 mice were harvested using institutionally approved protocols (UM UCUCA # 8518) and cleansed of soft tissue. If not tested immediately, the specimens were wrapped in gauze soaked in calcium buffered saline and stored at -30 °C before mechanical testing. Specimens were thawed prior to mechanical testing.

To prepare the femora for mechanical testing the condyles were embedded in a cold setting acrylic. The acrylic ends were shaped to allow the condyles of the femur to be encapsulated by the acrylic and to provide a rod by which the specimen could be fixed in the mechanical testing apparatus while minimizing the effects of the gripping forces. A custom-made fixture consisting of a metal bar with a milled groove was used to properly align the specimen with the embedded ends to provide a straight gauge length of bone tissue. The exposed section was kept moist with gauze soaked in calcium buffered saline.

The specimens were loaded in a custom-made dynamic mechanical tester, which was designed to work with our Raman microprobe (Figure 1). A stepper motor and lead screw allow crosshead positioning to $\pm 0.2 \mu\text{m}$. A load cell (Transducer Techniques, Temecula, CA) rated for 44 Newtons with repeatability of measurement to better than 0.01 Newtons was used to measure the applied load. The load cell was placed in line with the moving rod. Collet-style grips were used to secure the specimen in the test apparatus. The collets were attached to rods that were allowed to rotate freely to minimize torsional loads on the specimens and were threaded to accommodate specimens of various lengths. This mechanical tester was modified from the one used in our previous experiments to allow compression to be applied to the specimens as well as tension. All experiments were performed under displacement control. Specimens were kept moist by dripping calcium buffered saline on the specimens during the experiments.

The 785 nm Raman microprobe employs an attenuated beam of a Kaiser Invictus laser and an epi-illumination geometry as previously described.³² Laser light was focused onto the middle of the shaft of the specimen using a Leica 5X, 0.12 NA objective, providing 160 mW using a line focus. The Raman scattered light was collected by the same objective and focused into a Kaiser Optical Systems (Ann Arbor, MI) Holospec (f/1.8) spectrograph and collected on a thermoelectrically cooled, back-thinned deep depletion CCD detector. Spectra were integrated for 240 seconds. The load on the specimen was measured at the beginning and end of each integration. The load cell measurements were averaged to provide a single load measurement for each spectrum collected. All measurements were made at room

temperature (21 C +/- 1). A transect or line consisting of 128 spectra was collected parallel to the diaphysis, mid femur.

The wavenumber calibration, image curvature correction, baseline correction, and selection of subregions in the spectral datasets were performed in Matlab 6.1 (The Math Works, Natick, MA) using built-in and locally-written scripts. Peak fitting calculations were performed in GRAMS/AI 7.01 (ThermoGalactic). Because bone is highly scattering, data were collected from entire CCD frames collected and corrected for image curvature and all spectra in the frame were averaged.

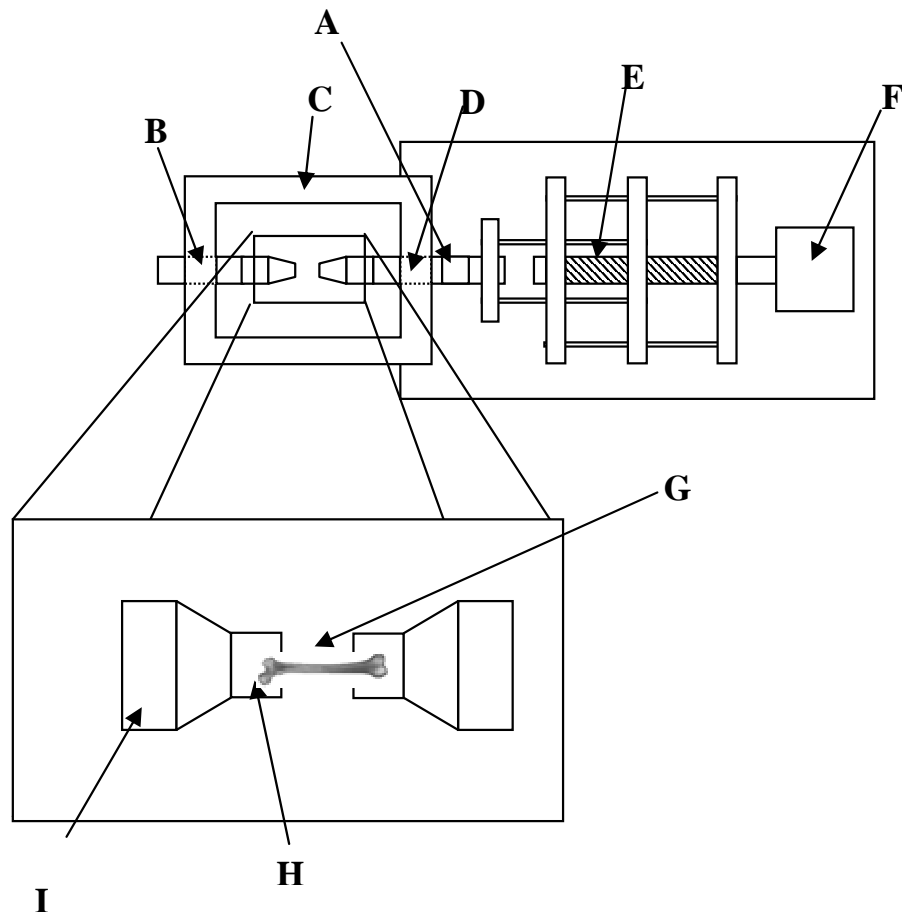


Figure 1: Schematic of dynamic mechanical testing apparatus (A) load cell, (B) fixed rod, (C) sample compartment, (D) movable rod, (E) lead screw, (F) stepper motor, (G) collet, (H) embedded end of murine femur, (I) bone specimen

From this and previous experiments the exposed length of the femur is approximately 10 mm. The cross section of the femur, approximated as an elliptical ring, has a major axis ranging between 2.13 and 2.3 mm and a minor axis ranging between 1.38 to 1.70 mm. The ring thickness ranges from 0.23 mm to 0.33 mm. The cross sectional areas range from 1.0mm² to 1.7 mm², making 1 Newton between 0.6 and 1 MPa across the cross section of the tissue. The cross-head position was changed by 2 microns per spectrum increasing the tensile strain on the specimen by approximately 200 microstrain per spectrum.

3. RESULTS

A murine femur was first loaded in tension with approximately 3 Newtons of force, then the lead screw was reversed, first releasing the tension and then compressing the femur with approximately 1.5 Newtons of force. Spectra were obtained with 240 seconds of integration time. The spectra were then segmented into smaller sub regions and baseline corrected with a third order polynomial to remove the fluorescence background. Spectra were collected after each change in the cross head positions.

The sub region taken for the mineral bands in the spectra was between 870 cm^{-1} and 1150 cm^{-1} to include both the dominant phosphate ν_1 band and the smaller carbonate ν_1 / phosphate ν_3 bands. The sub region selected to examine the amide III band was between 1120 cm^{-1} and 1550 cm^{-1} . The phosphate ν_1 band envelope was fit to two (2) Voigt bands one with a center ca. 945 cm^{-1} and the other with a center ca. 956 cm^{-1} . The amide III band envelope was fit to three Voigt bands, one with a center ca. 1200 cm^{-1} , the second with a center ca. 1230 cm^{-1} and the third with a center ca. 1260 cm^{-1} .

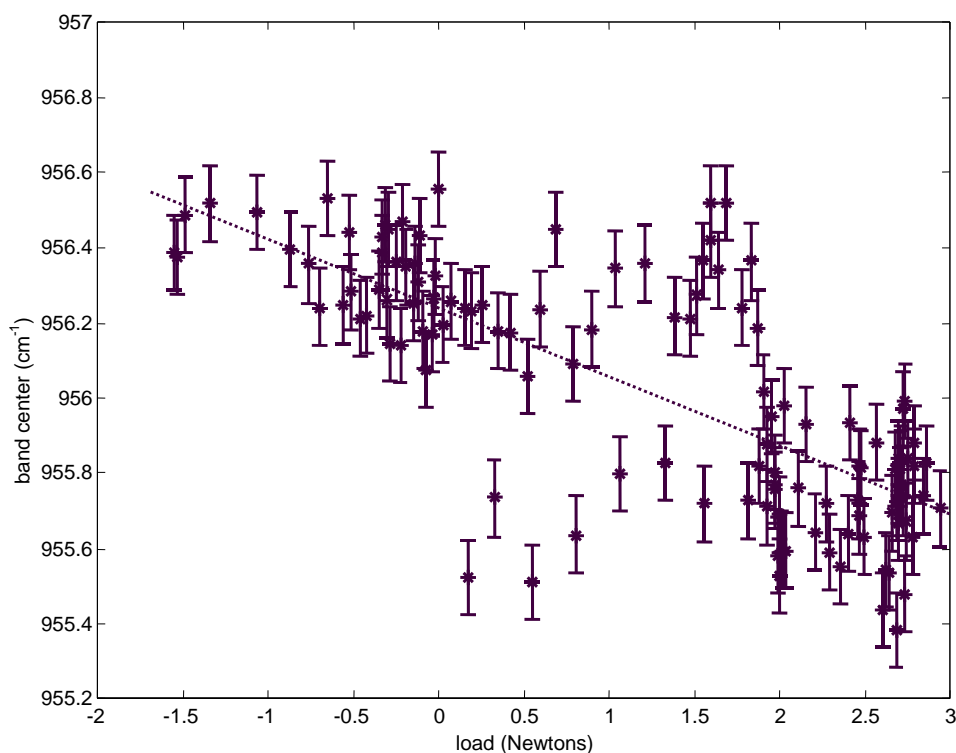


Figure 2: Plot of the band center for the main phosphate ν_1 band in the ca. 960 cm^{-1} band envelope. A strong correlation to a linear fit is found ($R^2=0.56$, $p<<0.05$). Negative load values represent compressive loads, positive load values represent tensile loads.

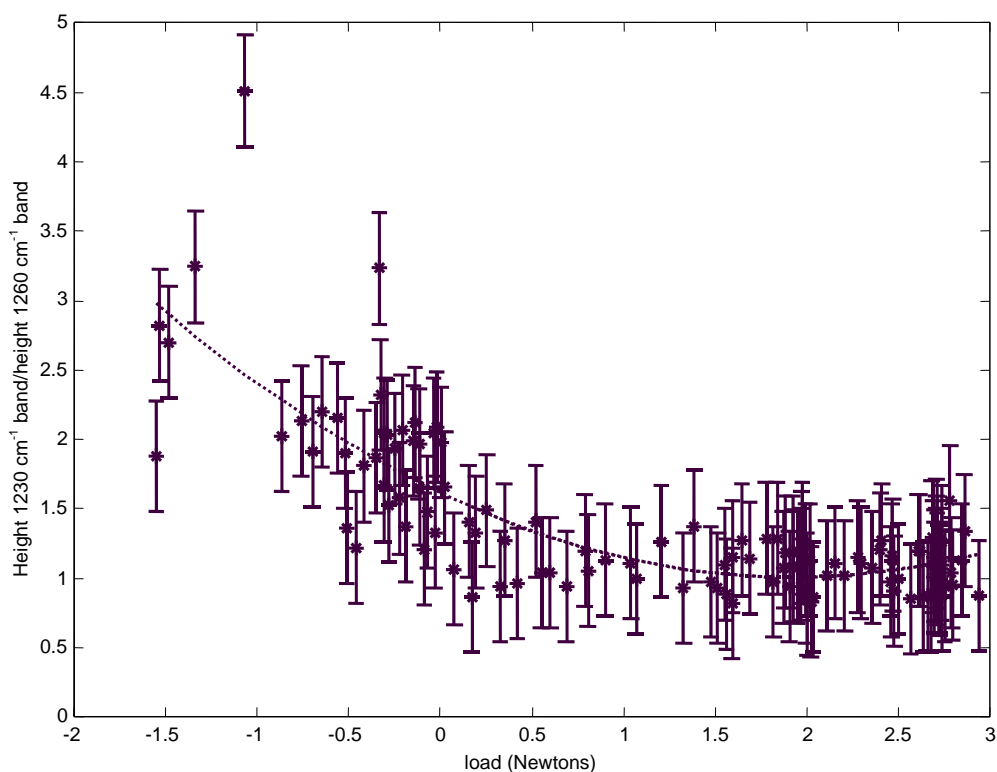


Figure 3: Plot of the relative height of the ca. 1230 cm^{-1} band to the height of the ca. 1260 cm^{-1} band in the amide III band envelope. A strong correlation to a quadratic fit is found ($R^2=0.65$, $p<<0.05$). Negative load values represent compressive loads, positive values represent tensile loads.

A plot of the band center versus load for the ca. 956 cm^{-1} phosphate ν_1 band (Figure 2) shows a clear decrease in the peak center of the band as a function of load magnitude. The ratio of the heights of the ca. 1230 cm^{-1} to and the ca. 1260 cm^{-1} bands in the amide III envelope fit best to a quadratic dependence on load.

4. DISCUSSION

We have chosen to examine fresh, intact tissue specimens for several reasons. Specimens used for mechanical testing are often fixed, dehydrated and/or milled to standard shapes and sizes. While for many materials this is advantageous because it removes some potential variables in the experiments, these procedures may potentially generate artifacts or change the molecular composition of the tissue. The dimensions of an intact mouse femur are also already compatible with the design of a small mechanical testing device that can be mounted on a Raman microprobe.

Pressure effects on the structure and vibrational spectra of inorganic crystals have been widely studied, primarily by geologists.³³ Compression and/or decrease in temperature of simple ionic crystals results in cations and anions in the lattice moving closer together but has less effect on the internal dimensions and geometry of small oxy-anions, as the lattice modulus is about 1/3 that of the phosphate modulus.^{34,35} Reducing pressure (where practical) or increasing the temperature of the crystal moves ions farther apart. Idealized models can be used to relate observed spectral band shifts and widths to structure changes. Linearity is often observed over wide pressure ranges and in some cases band shifts are directly related to heat capacity, which also depends on expansion/compression of the lattice. To a good first

approximation for an ionic crystal the pressure dependence of a vibrational band of frequency $\bar{\nu}_i$ can be described³³ by equation 1, the Grüneisen parameter.³⁶

$$\gamma_{iT} = \frac{K_T}{\bar{\nu}_i} \left[\frac{\partial \bar{\nu}_i}{\partial P} \right]_T \quad (1)$$

In equation 1, γ_{iT} is the pressure coefficient of the vibration and K_T is the bulk modulus of the material. In the simplest case oxyanion internal coordinates do not change and there are no contributions from hydrogen bonding or other weak forces. The inter-ion spacing in the crystal depends on the balance between a long range attractive force and a short range repulsive force. Then γ_{iT} is a constant, approximate value 2.2. This form of the equation is strictly valid only for hydrostatic pressure. If the linearity in $d\nu/dP$ is observed under other modes of loading, this would infer that ionic spacing is altered under load.

The response is clear, under tensile loading the phosphate ν_1 band center increases under compression. The observed change in band center is $-0.18 \text{ cm}^{-1}\text{N}^{-1}$. This value compares favorably with our previous changes observed under tensile loading alone²⁴ and the values are about an order of magnitude larger than the values from the high pressure Raman studies.²³ This larger shift may have several causes. The forces experienced by individual mineral crystallites may be larger than the forces calculated from the applied engineering load and the tissue specimen dimensions because of the ultrastructural architecture of bone material. The tissue contains collagen fibrils that are covalently cross-linked and void spaces filled with water. Voytik-Harbin et al. report that only a portion of the cross sectional area of collagen containing tissues and tissue derived materials that they have observed is accounted for by the cross sections of the collagen fibrils themselves.³⁷ This means that individual fibrils and crystallites may be experiencing larger stresses than those calculated from macroscopic forces and bone tissue specimen dimensions.

We observe an approximately linear response between change in pressure (force/unit area) and frequency, which may be distorted by the viscoelastic properties of bone. It is also important to note that bone mineral crystallites are highly substituted, small,^{30,38} and synthetic B-type carbonated apatites of similar composition to bone are only 1-3 unit cell widths in their smallest dimensions³⁹. Such small crystals may not behave in a manner that is well described when compared to a perfect, infinite crystal lattice.

The extensive literature describing the use of vibrational spectroscopy to determine the secondary conformation of proteins spans several decades.^{40-44, 45-48} In general, the position and shape of the backbone amide bands are indicative of protein structure, as summarized in a recent review by Pelton and McLean.⁴⁸ Bandekar describes the different amide modes existent in several standard protein secondary structures, their corresponding infrared and Raman band positions, and provides a description of several specific methods for studying protein conformation.⁴⁹

At the same time that the phosphate ν_1 band is observed to change, a clear change in the relative heights of the ca. 1230 cm^{-1} and ca. 1260 cm^{-1} are observed under mechanical loading. There is a pronounced decrease in the the height of the ca. 1260cm^{-1} band and a small increase in the height of the ca 1230 cm^{-1} band. This change is more pronounced in the compressive loading regime than when the specimen is undergoing tensile loading. This change can be explained by changes in the shape of the collagen backbone as the bone tissue is mechanically loaded. Carden observed in earlier experiments in demineralized bone tissue that there was a change in the center of gravity of the amide III band envelope when the demineralized bovine bone tissue was loaded in tension⁵⁰. The change in relative intensities of the components of the band envelope would certainly cause the center of gravity of the band envelope to change. Whether these changes are truly most pronounced in compression or if changes can be seen under larger tensile forces is a focus of current experiments. The minimum of the quadratic fit is not located at 0 N where it might be expected. Rather it is located close to 2 N. This finding suggests that bone tissue under compressive stress.

5. CONCLUSIONS

The band center of the phosphate ν_1 band was observed to change with mechanical load. A change of $-0.18 \text{ cm}^{-1} \text{ N}^{-1}$ was observed for a murine femur loaded both in tension and in compression. This is equivalent to a change of $-0.18 \text{ cm}^{-1} \text{ N}^{-1}$ to $0.3 \text{ cm}^{-1} \text{ N}^{-1}$ when the femur is loaded from 3 N in tension to 1.5 Newtons in tension. At the same time a change is observed in the relative heights of two components of the amide III band envelope. The ca. 1230 cm^{-1} band increases in height relative to the ca. 1260 cm^{-1} band as the femur is loaded. That changes are observed in the spectra during dynamic loading further supports our earlier conclusion that changes observed in bone are truly a function of the applied mechanical load and not preexistent in the material.²²

Both the inorganic mineral and the protein matrix clearly play an important role in the dynamic response of bone tissue to elastic mechanical stress in a physiological range. The classical view that bone mineral simply provides mass and stiffness to the mechanical properties of bone tissue is only good to a first approximation and must be revised to include the dynamic changes in the individual components.

ACKNOWLEDGEMENTS

The authors gratefully acknowledge financial support from the following sources: the University of Michigan Bone Research Core Center (NIH grant P30 AR46024), and DoD/Department of the Army DAMD17-03-1-0556.

REFERENCES

1. R. J. Young and X. Yang, "Interfacial failure in ceramic fibre/glass composites.," *Composites Part A* **27A**, pp. 737-741, 1996.
2. Y. Yukawa, K. Saki, and T. Ogawaq, "Measurement of stress distribution inside crystals by multichannel Raman scattering tomography," *Solid-State Electron.* **43**, pp. 1195-1199, 1999.
3. A. Kailer, K. G. Nickel, and Y. G. Gogotsi, "Raman microspectroscopy of nanocrystalline and amorphous phases in hardness indentations," *J. Raman Spectrosc.* **30**, pp. 939-946., 1999.
4. I. I. Vlasov, V. G. Ralchenko, E. D. Obratsova, A. A. Smolin, and V. I. Konov, "Analysis of intrinsic stress distributions in grains of high quality CVD diamond film by micro-Raman spectroscopy," *ThinSolid Films* **308**, pp. 168-172, 1997.
5. W. Y. Yeh and R. J. Young, "Deformation processes in poly(ethylene terephthalate) fibers," *Journal of Macromolecular Science* **B37**, pp. 83-118, 1998.
6. M. L. Mehan and L. S. Schadler, "Micromechanical behavior of Short-Fiber Polymer Composites.," *Composites Science and Technology* **60**, pp. 1013-1026, 2000.
7. J. C. Rodriguez-Cabello, J. C. Merino, T. Jawhari, and J. M. Pastor, "Rheo-optical Raman study of chain deformation in uniaxially stretched bulk isotactic polypropylene.," *J. Raman Spectrosc.* **27**, pp. 463-467, 1996.
8. J. Xu, D. F. R. Gilson, I. F. Butler, and I. Stangel, "Effect of high external pressures on the vibrational spectra of biomedical materials: calcium hydroxyapatite and calcium fluoroapatite.," *Journal of Biomedical Materials Research* **30**, pp. 239-244, 1996.
9. An, Y. H. ; Draughn, R. A. *Mechanical Testing of Bone and the Bone-Implant Interface*; CRC Press: Boca Raton, Fl., 2000.
10. A. L. Boskey, "Mineral-matrix interactions in bone and cartilage," *Clinical Orthopaedics and Related Research* **281**, pp. 244-274, 1992.
11. D. Taylor, F. O'Brien, A. Prina-Mello, C. Ryan, P. O'Reilly, and T. C. Lee, "Compression data on bovine bone confirms that a "stressed volume" principle explains the variability of fatigue strength on results," *Journal of Biomechanics* **32**, pp. 1199-1203, 1999.
12. A. Ascenzi and E. Bonucci, "The tensile properties of single osteons," *Anatomical Record* **158**, pp. 375-386, 1967.

13. T. E. Wenzel, M. B. Schaffler, and D. P. Fyhrie, "In vivo trabecular microcracks in human vertebral bone," *Bone* **19**, pp. 89-95., 1996.
14. R. B. Martin, V. A. Gibson, S. M. Stover, J. C. Gibeling, and L. V. Griffin, "Residual strength of equine bone is not reduced by intense fatigue loading: implications for stress fracture.," *Journal of Biomechanics* **30**, pp. 109-114., 1997.
15. Y. H. An, J. Zhang, Q. Kang, and R. J. Friedman, "Mechanical properties of rat epiphyseal cancellous bones studied by indentation testing," *J. Mater. Sci.* **8**, pp. 493-495, 1997.
16. D. R. Sumner, T. L. Willke, A. Berzins, and T. M. Turner, "Distribution of Young's modulus in the cancellous bone of the proximal canine tibia," *Journal of Biomechanics* **27**, pp. 1095-1099., 1994.
17. S. Saitoh, Y. Nakatsuchi, L. Latta, and E. Milne, "An absence of structural changes in the proximal femur with osteoporosis.," *Skeletal Radiology* **22**, pp. 425-431, 1993.
18. Y. H. An, Q. Kang, and R. J. Friedman, "Mechanical symmetry of rabbit bones studied by bending and indentation testing.," *American Journal of Veterinary Research* **57**, pp. 1786-1789, 1996.
19. J. Timlin, A. Carden, M. D. Morris, and D. H. Kohn, "Raman Spectroscopic Imaging Markers for Fatigue-Related Microdamage in Bovine Bone," *Anal. Chem.* **72**, pp. 2229-2236, 2000.
20. M. D. Morris, A. Carden, R. M. Rajachar, and D. H. Kohn, "Bone microstructure deformation observed by Raman microscopy," *Proceedings of the SPIE* **4254**, pp. 81-89, 2001.
21. M. D. Morris, A. Carden, R. M. Rajachar, and D. H. and Kohn, "Effects of Applied Load on Bone Tissue as Observed by Raman Spectroscopy," *Proceedings SPIE* **4614**, pp. 47-54, 2002.
22. A. Carden, R. M. Rajachar, M. D. Morris, and D. H. Kohn, "Ultrastructural changes accompanying the mechanical deformation of bone tissue: a Raman imaging study," *Calcif. Tissue Int.* **72**, pp. 166-175, 2003.
23. Morris, M. D.; de Carmejane, O.; Carden, A.; Davis, M. K.; Stixrude, L.; Tecklenburg, M.; Rajachar, R. M.; Kohn, D. H. *Proc. SPIE*, **4958**, pp. 88-97, 2003.
24. M. D. Morris, W. F. Finney, R. M. Rajachar, and D. H. Kohn, "Bone tissue ultrastructural response to elastic deformation probed by Raman spectroscopy," *Faraday Discussions* **126**, pp. 159-168, 2004.
25. G. H. Nancollas, M. Lore, L. Perez, C. Richardson, and S. J. Zawacki, "Mineral phases of calcium phosphate," *Anatomical Record* **224**, pp. 234-241, 1989.
26. A. Carden and M. D. Morris, "Application of vibrational spectroscopy to the study of mineralized tissues," *Journal of Biomedical Optics* **5**, pp. 259-268., 2000.
27. G. Penel, G. Leroy, C. Rey, and E. Bres, "MicroRaman spectral study of the PO₄ and CO₃ vibrational modes in synthetic and biological apatites," *Calcif. Tissue Int.* **63**, pp. 475-481, 1998.
28. B. G. Frushour and J. L. Koenig, "Raman scattering of collagen, gelatin and elastin.," *Biopolymers* **14**, pp. 379-391, 1975.
29. R. B. Martin and D. L. Boardman, "The effects of collagen fiber orientation, porosity, density, and mineralization on bovine cortical bone bending properties. " *Journal of Biomechanics* **26**, pp. 1047-1054, 1993.
30. W. J. Landis, K. J. Hodgens, J. Arena, M. J. Song, and B. F. McEwen, "Structural relations between collagen and mineral in bone as determined by high voltage electron microscopic tomography," *Microscopy Research and Technique* **33**, pp. 192-202, 1996.
31. J. D. Currey, "The effect of porosity and mineral content on the Young's modulus of elasticity of compact bone.," *Journal of Biomechanics* **21**, pp. 131-139, 1988.
32. K. Christensen and M. D. Morris, "Hyperspectral Raman microscopic imaging using Powell lens line illumination," *Appl. Spectrosc.* **52**, pp. 1145-1147, 1998.
33. P. Gillet, R. J. Hemley, and A. McMillan, "Vibrational properties at high pressures and and temperatures," *Rev. Mineralogy* **37**, pp. 525-590, 1998.
34. P. Comodi, Y. Liu, P. F. Zanazzi, and M. Montagnoli, "Structural and vibrational behavior of fluorapatite with pressure. Part I. in situ single-crystal x-ray diffraction investigation," *Phys. Chem. Minerals* **28**, pp. 219-224, 2001.
35. P. Comodi, Y. Lin, and M. L. Frezzotti, "Structural and vibrational behaviour of fluorapatite with pressure. Part II: in situ micro-Raman spectroscopic investigation," *Phys. Chem. Minerals* **28**, pp. 225-231, 2001.
36. Hemley, R. J. *Ultrahigh-Pressure Mineralogy: Physics and Chemistry of the Earth's Deep Interior*; Mineralogical Society of America: Washington, D. C. 1998.
37. S. L. Voytik-Harbin, B. A. Roeder, J. E. Sturgis, K. Kokini, and J. P. Robinson, "Simultaneous mechanical loading and confocal reflection microscopy for three dimensional microbiomechanical analysis of

- biomaterials and tissue constructs," *Microscopy and Microanalysis* **9**, pp. 74-85, 2003.
38. V. Ziv and S. Weiner, "Bone crystal sizes - a comparison of transmission electron-microscopic and X-Ray-Diffraction line-width broadening techniques," *Connective Tissue Research* **30**, pp. 165-175, 1994.
39. T. I. Ivanova, O. V. Frank-Kamenetskaya, A. B. Kol'tsov, and V. L. Ugolkov, "Crystal structure of calcium deficient carbonated hydroxyapatite. Thermal decomposition," *J. Solid State Chem.* **160**, pp. 340-349, 2001.
40. D. Garfinkel and J. T. Edsall, "Raman spectra of amino acids and related compounds. 10. The Raman spectra of certain peptides and of lysozyme," *J. Am. Chem. Soc.* **80**, pp. 3818, 1958.
41. Yu. N. Chirgadze and N. A. Nevskaya, "Infrared Spectra and Resonance Interaction of Amide I Vibration of the Parallel-Chain Pleated Sheet," *Biopolymers* **15**, pp. 627-636, 1976.
42. Yu. N. Chirgadze, E. V. Brazhnikov, and N. A. Nevskaya, "Intramolecular Distortion of the α -helical Structure of Polypeptides," *J. Mol. Biol.* **102**, pp. 781-792, 1976.
43. J. T. Pelton and L. R. McLean, "Spectroscopic methods for analysis of protein secondary structure," *Anal. Biochem.* **277**, pp. 167-176, 2000.
44. V. Renugopalakrishnan, L. A. Carreira, T. W. Collette, J. C. Dobbs, G. Chandraksasan, and R. C. Lord, "Non-uniform Triple Helical Structure in Chick Skin Type I Collagen on Thermal Denaturation: Raman Spectroscopic Study," *Z. Naturforsch., C: Biosci.* **53**, pp. 383-388, 1998.
45. J. Xu, D. F. R. Gilson, and I. S. Butler, "FT-Raman and high pressure FT-infrared spectroscopic investigation of monocalcium phosphate monohydrate, $(\text{Ca}(\text{HPO}_4)_2 \cdot \text{H}_2\text{O})$," *Spectrochimica Acta* **54A**, pp. 1869-1878, 1999.
46. Yu. N. Chirgadze and N. A. Nevskaya, "Infrared Spectra and Resonance Interaction of Amide I Vibration of the Parallel-Chain Pleated Sheet," *Biopolymers* **15**, pp. 627-636, 1976.
47. V. Renugopalakrishnan, L. A. Carreira, T. W. Collette, J. C. Dobbs, G. Chandraksasan, and R. C. Lord, "Non-uniform Triple Helical Structure in Chick Skin Type I Collagen on Thermal Denaturation: Raman Spectroscopic Study," *Z. Naturforsch., C: Biosci.* **53**, pp. 383-388, 1998.
48. J. T. Pelton and L. R. McLean, "Spectroscopic Methods for Analysis of Protein Secondary Structure," *Anal. Biochem.* **277**, pp. 167-176, 2000.
49. J. Bandekar, "Amide Modes and Protein Conformation," *Biochim. Biophys. Acta* **1120**, pp. 123-143, 1992.
50. Carden, A. University of Michigan, Ann Arbor, Michigan, 2002.